EXPERIMENTAL STUDY OF A SINGLE PHASE FLOW IN A PIPE SEPARATOR

EYITAYO A. AFOLABI[1] & J. G. M. LEE[2]
[1]Department of Chemical Engineering,
Federal University of Technology, Minna, Nigeria.
[2]Newcastle University, Newcastle upon Tyne, UK.
E-mail: elizamos2001@yahoo.com Phone No: +234-807-220-1514

Abstract

An experimental investigation of the hydrodynamic behaviour of a single water flow was performed on a laboratory scale model of a three phase pipe separator. The velocity distributions of swirling flow were measured using the Stereoscopic-Particle Image Velocimetry technique at three different axial positions within the pipe separator. The results show that the shapes of the tangential velocity profiles are independent of axial positions within the pipe separator and the magnitude of the mean tangential velocity decreases moving away from the inlet section to the outlets. The axial velocity measurements show the presence of fluid dynamic instabilities such as vortex breakdown and precessing vortex core caused by the high swirling motion inside the pipe separator.

Keywords: Stereoscopic Particle Image Velocimetry, Pipe Separator, Velocity Profile

Introduction

In the past, the multiphase separation technology used in the oil and gas industry has been based on conventional vessel-type separators which are expensive, heavy and bulky in size. Nowadays, compact separators are widely used as an effective and economical alternative to conventional separators especially in offshore platforms in oil and gas production operations (Erdal, 2001). The choice of this technology is because it is simpler to operate, more lightweight, has neither moving nor internal parts, requires less floor space, and involves lower capital and operational costs (Vazquez, 2001).

A pipe separator is a device that spins a continuous phase stream to remove entrained dispersed phases by centrifugal force (Erdal, 2001). It operates at velocities where the flow is found to be typically turbulent and often characterized with flow reversal, flow separation and three-dimensional boundary layers with strong streamline curvature (Leeuwner & Eksteen, 2008; Slack & Wraith, 1997). Cylindrical cyclone or pipe separator has potential application as a free water knockout system in equipment for the upstream oil and gas production. This includes down-hole, surface (onshore and offshore) and subsea separation. Other applications include, use in flare gas scrubbers, slug catchers and portable well testing equipment. Preliminary studies have shown that the three phase pipe separator is an effective device use for partial separation of air-oil-water mixtures at moderate velocities (Vazquez, 2001). However, the cylindrical cyclone operates as a mixer rather than separator at high velocities.

As shown in Figure 1, the three phase pipe separator consists of a tangential inlet inclined at an angle of 27^o to the vertical cylindrical body and an oil finder which is an inner concentric pipe extended through the bottom. The air-oil-water mixture enters through the inclined inlet designed to promote the pre-separation of the gas-liquid mixture. The tangential inlet with reduced area produces a swirling motion in the vertical cylindrical pipe. The gas flows upwards to the gas outlet and leaves the single system compact separator. The liquid-liquid mixture moves to the lower section of the vertical pipe. As a result of differences in density, the centrifugal effect segregates the oil-water mixture, thereby concentrating the oil at the center of the pipe whereas the water moves towards the wall region. The oil rich core formed at the center flows through the oil finder and the water rich fraction flows to the annulus between the pipe wall and the oil finder, leaving the single stage three phase separator through the water-rich outlet (Afolabi, 2012; Vazquez, 2001). Stereoscopic Particle Image Velocimetry (SPIV) is a new non-intrusive visualization experimental technique which is ideally suited to determining the whole field three-dimensional fluid velocity in a pipe separator. Stereoscopic PIV allows the determination of mean velocity and detailed turbulence quantities such as Reynolds stresses. One of the first attempts to measure the velocities in a cylindrical cyclone using Stereoscopic PIV was presented by Liu *et al* (2006). They investigated the swirling flow structure in a gas cyclone by measuring the instantaneous whole field tangential, axial and radial velocities of air flow. The time-averaged tangential velocity profile showed that the tangential velocity of the gas generated an inner quasi-forced vortex and outer quasi-free vortex. The axial velocity profile revealed an inner upward flow and outer downward flow. They further observed a reverse flow at the inner core of the forced vortex around the cyclone axis. This flow reversal is generated by the motion of precessing vortex core (PVC), which is usually associated with vortex breakdown and insurgence of reverse flow.

The work of Vasquez (2001) did not provide the hydrodynamic flow behaviour of the complex, swirling and turbulent flow in the three-phase pipe separator. This is the main focus that this research work is going to address. Previous study by Erdal (2001) was limited to a Laser Doppler Velocimetry measurement of a single phase flow that passed through a cyclone with a single outlet. However, this research work is aimed at providing SPIV measurement of single flow passing through three different outlets of a pipe separator. A lack of understanding of the complex flow behaviour within the three-phase cylindrical cyclone prevents complete confidence in its design.

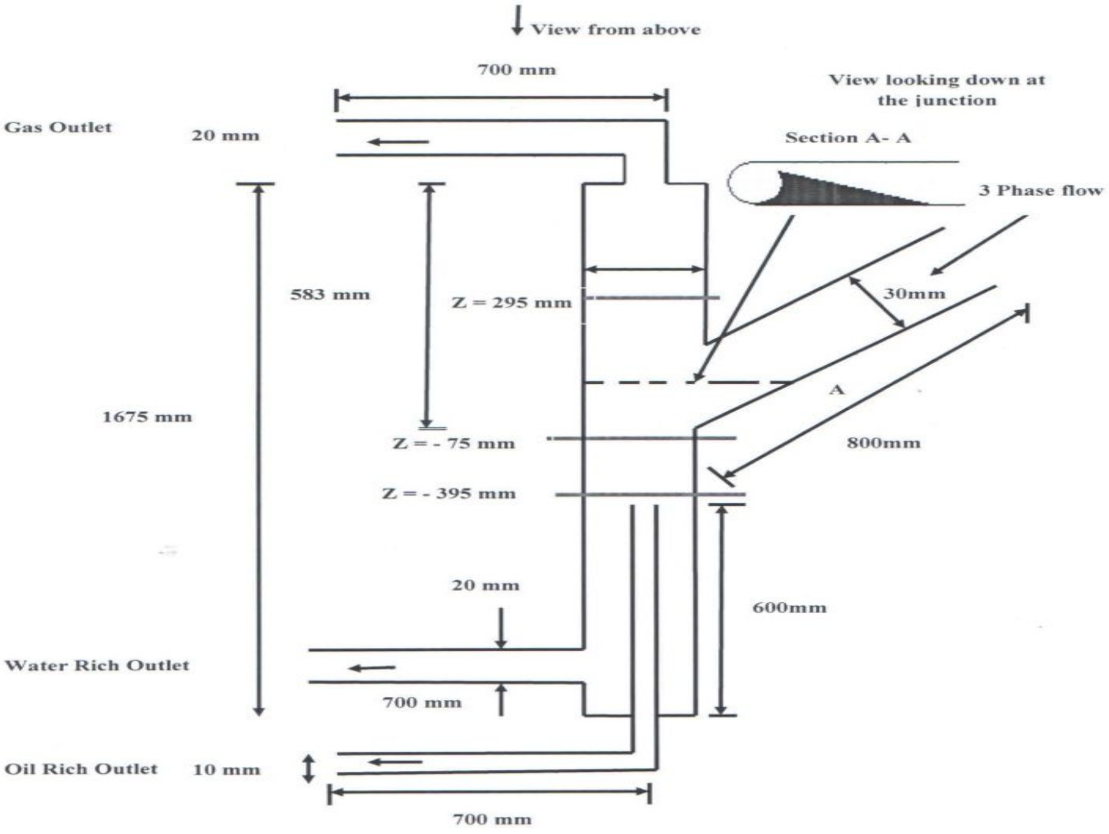

Figure 1: Single Stage Three-Phase Cylindrical Cyclone System (Afolabi, 2012)

Detailed investigation of the hydrodynamic flow behaviour will allow the correct prediction of separation performance, which is necessary for improved design in its applications. The present work focuses on investigating the hydrodynamic behaviour of a single phase flow within the three phase pipe separator using Stereoscopic (PIV) technique.

Methodology

Experimental Facility and Flow Loop: The three phase flow facility used in this study is based on one of the geometries developed and patented for multiphase flow separation by the Separation Technology Project of the University of Tulsa, USA. A 30 mm ID laboratory prototype of a three phase pipe separator was fabricated at School of Chemical Engineering and Advanced Material, Newcastle University, UK to investigate the hydrodynamic behaviour of the turbulent flow and separation efficiency. The separator test section was constructed using a transparent perspex tube. The single phase flow experiment was run with a water flow rate of 196 cm^3/s. The outlets were restricted with rubber bungs such that the percentage of water as a fraction of the inlet mass flow was 60 % through the air outlet, 33 % through the water-rich outlet and the balance through the oil-rich outlet (Afolabi, 2012).

S-PIV Set-up: The stereo-PIV system used for this investigation was manufactured by TSI Inc and loaned from the Engineering and Physical Sciences Research Council (EPSRC) engineering instruments pool. The single phase water flow was seeded with light reflecting Silver coated hollow glass spheres marketed by TSI Inc (10089-SLV). This seeding material has very good fluid and imaging properties for the current experiment (Melling, 1997). A CFR-200 double pulsed Nd: YAG laser system designed by Big Sky Laser was used as the light source to illuminate the tracer particles in the measurement plane. As shown in Figure 2, the laser beam passed through a TSI Model 610015 light arm, which helped in aligning the beam to the arm's optical axes so that the beam was not clipped but transmitted properly.

Two TSI Model 630059 POWERVIEW TM Plus 4MP PIV cameras with CCD sensors were installed on the Scheimpflug mounts so as to satisfy the stereoscopic camera condition. The two cameras looked at angle of $+45^o$ and -45^o to the light sheet. By tilting the image sensor plane and the lens principle to the Scheimpflug condition, the plane best of focus could be found so that it was aligned with the lightsheet (Prasad, 2000). These cameras were positioned at both sides of the light sheet in order to capture two exposures of the illuminated plane and then connected to a 64 bit frame grabber to subsequently transfer to a computer for automatic analysis using cross correlation method. A TSI 610035 laser pulse synchronizer was used to synchronize the image capturing and laser pulses. A water prism of 45 degrees was constructed and moved to the test section of the experimental rig in order to minimize optical distortion arising from refraction through the perspex wall. Two hundred pairs of images were recorded by the acquisition system at each measuring location. The software INSIGHT 3G from TSI Inc was used to controlled the hardware while capturing, retrieving and processing raw images in order to gain data on velocity vector fields.

Camera Calibration

A single plane calibration target populated by a Cartesian grid of 2 mm white marker dots with a 3 mm cross at the centre on a black background was cut to size to fit into the test section. The calibration target was moved using a micrometer in seven steps of 0.5 mm and images of the target were recorded and analysed by perspective calibration method of INSIGHT 3G software. The calibration image analysis produced a set of calibration points used to create a calibration mapping function, which was then used to combine 2-D PIV vector fields in order to obtain the three-dimensional vector field (Prasad and Jensen, 1995).

Results and Discussion

The experimental data presented were extracted along the y=0 line at three axial positions Z= -395, -75 and 295 mm of the pipe separator, as shown in Figures 1 and 3.

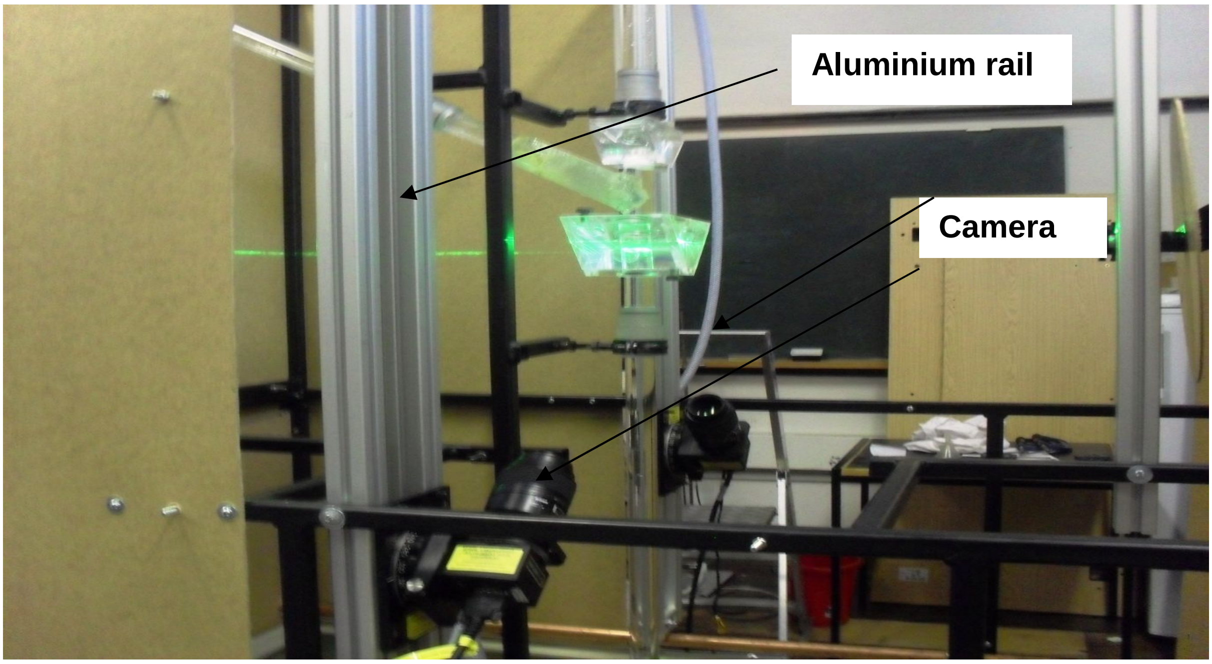

Figure 2: S-PIV Experimental Set-up

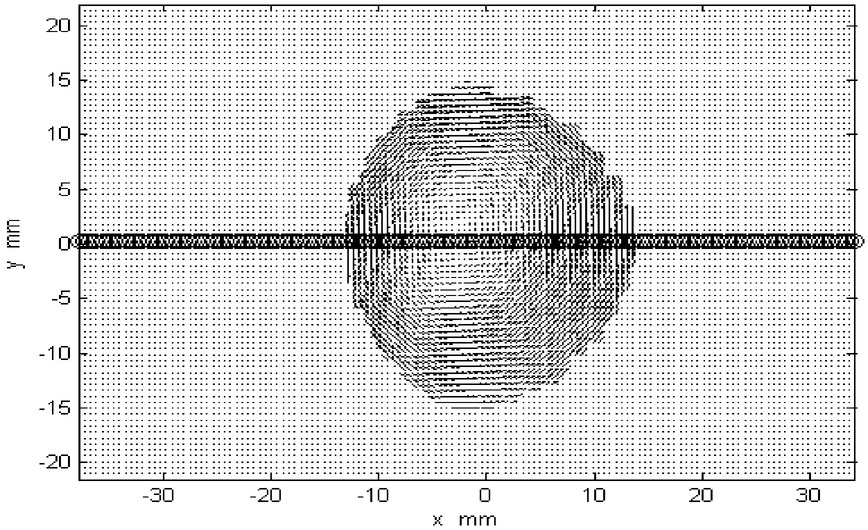

Figure 3: Experimental Data: Position of y=0 Sections

Tangential Velocity

Figure 4 shows the comparison of the mean tangential velocities of the water flow at the Z=- 395, -75 and 295 mm axial positions. It can be observed that the tangential velocity at all axial positions increases moving away from the center of the tube before reaching a maximum and then dropping close to the wall due to wall friction. At Z=295 mm, the maximum tangential velocity occurs at a radius of 7.5 mm. However, at Z=-395 mm the maximum velocity occurs at a radius of 10mm and at Z= -75 mm, maximum velocity is observed at a radius of 12.5 mm. By identifying this location, the tangential velocity

distribution can be described as a continuous flow stream with an outer and inner region. The inner region is characterized as a forced vortex where tangential velocity increases directly with radius. However, the outer region is characterized as a free vortex and the rate of rotation is greatest at the center and then decreases progressively (Kelsall, 1952).
This can be described by the relationship presented in equation 1;

$$v_\theta = Cr^n \qquad (1)$$

where v_θ is the tangential velocity, C is a constant of proportionality, and r is the radial coordinate of the vortex. For a forced vortex, n= 1 and a free vortex, n= -1. The observations made are similar to the reports of earlier researchers in the literature (Leeuwner and Eksteen, 2008; Slack and Wraith, 1997). At Z=-75 mm, the forced vortex extends over 75 % of the surface area of the separator's plane and decreases to 67% and 50% at Z= -395 mm and 295 mm respectively. However, the free vortex occupies 50% of the surface area of the separator's plane at Z=295 mm and decreases to 33.3 % and 25 % at the Z= -395 mm and -75 mm axial positions respectively. This means that the surface area occupied by the forced vortex decreases moving away from the inlet section. However, the free vortex increases when moving away from Z=-395 mm. The comparison of the tangential velocity profiles at the three axial positions shown in Figure 4 reveals that the surface area occupied by forced vortex decreases moving away from the inlet section. However, surface area occupied by free vortex increases when moving away from Z=-395 mm. The comparison of the tangential velocity profiles at the three axial positions shown in Figure 4 reveals that the magnitude of mean tangential velocity decreases as we move away from the inlet section towards the outlets. The reason for this is mainly the decay in swirl intensity as the flow moves away from the inlet. Therefore, as the fluid flow away from the inlet section, the tangential velocity gradually decreases and relatively less strong centrifugal fields are generated. Tangential velocity magnitude is a measure of the centrifugal force in the vortex region and this helps to improve the separation efficiency of the pipe separator.

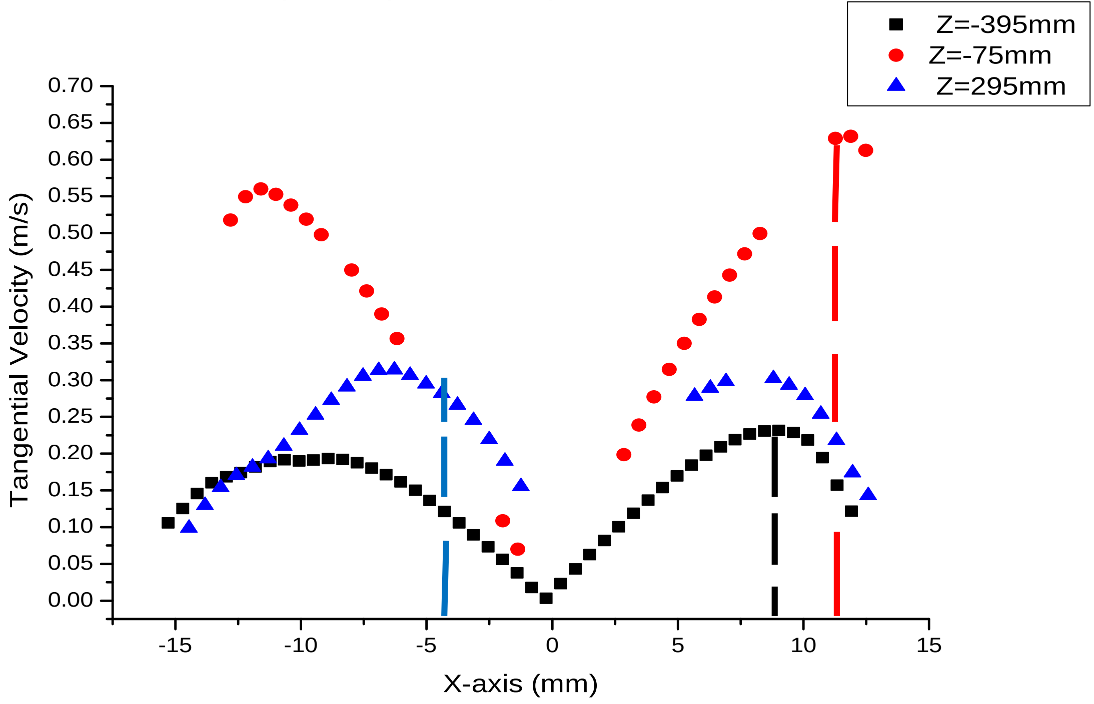

Figure 4: Comparison between the Tangential Velocity Profiles at Three Axial Positions in the Cyclone

It is generally accepted that tangential velocities are directly proportional to separation efficiencies. Therefore, most of the fluid separation occurs immediately at the region where the inlet section joins the vertical axis of the cyclone.

Axial Velocity

In agreement with other researchers such as Peng, *et al* (2002) and Monredon *et al* (1992), the positive axial velocity profile is hereby referred to as region of flow in an upward direction with respect to the rotation axis. A negative axial velocity profile will be taken as a region of flow in a downward direction from the rotation axis. The contour plot shown in Figure 5 reveals the existence of a region of recirculation or reverse flow at the center of the cyclone and a decreased axial velocity near the wall. The reverse flow refers to a region of positive axial velocity and is believed to be generated and dominated by the motion of a Precessing Vortex Core (PVC) usually defined as a time dependent instability that leads to vortex breakdown (Peng, *et al*, 2002; Yazdabadi *et al.*, 1994). Figure 6 shows the comparison between the axial velocity profiles at the three different axial positions in the separator. At Z=-395 mm and -75 mm, the positive values of axial velocity decrease with an increase in radial distance and reaches zero at some distance away from the center of the tube.

However, close to the separator wall, the axial velocity reaches a minimum and then increases. This is due to higher friction at the separator wall. Axial velocity profiles at Z= -395 and -75 mm reveal a combination of downward and upward flow patterns at the wall and center of the tube respectively. However, at Z=295 mm there is no negative axial velocity at any x-axis coordinate. As can be seen in Figure 6, a large amount of water flows in an upward direction at the center of the tube and in a downward direction near to the wall at Z=-75 mm. For example, the maximum positive and negative axial velocities are 0.175 m/s at Z=-75 mm.

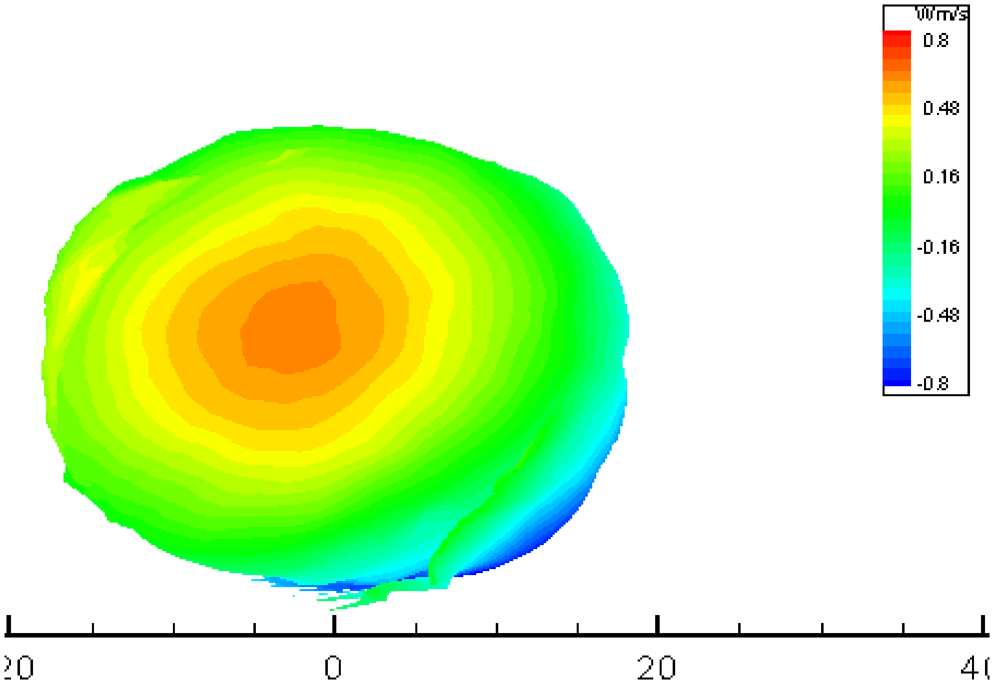

Figure 5: Contour Plot of the Axial Velocity at Z= -75 mm

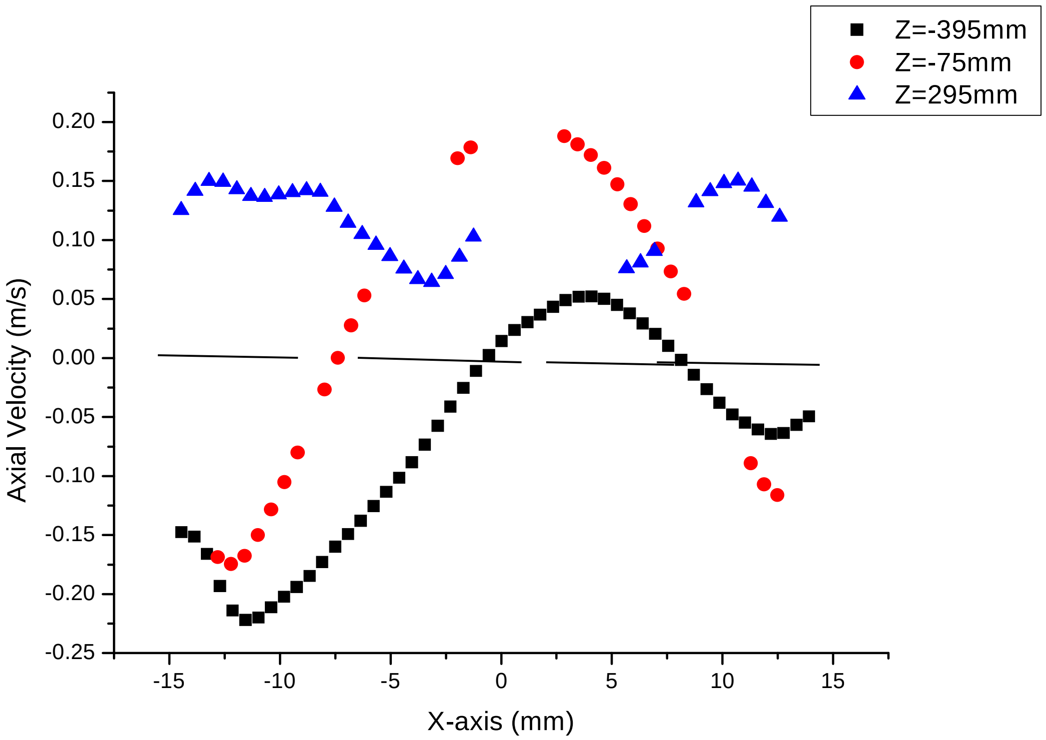

Figure 6: Comparison between the axial velocity profiles at three axial positions in the Cyclone

The maximum positive axial velocity among the three axial positions is 0.175 m/s at Z=-75 mm. At Z=-395 mm, a large downward flow is observed close to the wall together with small amounts of upward flow at the center of the tube. The location of the maximum axial velocity on the x-axis is at the center of the tube at Z=-75mm, but off center at Z= -395 mm. Similar observations of axial velocity flow patterns was made by Leeuwner and Eksteen (2008).

Radial Velocity

Figure 7 shows a graph of the comparison between the mean radial velocity profiles at the three axial positions in the cyclone. In agreement with other researchers such as Kelsall (1952) and Peng *et-al;* (2007), radial velocity flow is said to be directed inward when the radial velocity is negative and outward when its value is positive. As can be seen in Figure 7, radial flow is found to be inwards as we move away from the center of the tube at Z=$-395\ \mathrm{mm}$. However, close to the wall at the positive value of the x-axis, outward radial velocity begins to develop. At Z= $-75\ \mathrm{mm}$, radial velocity is observed to be directed outwards at all values of the x-axis. The radial velocity profile at Z= 295 mm shows inward flow as we move away from the center of the tube. However, close to the wall at a negative value of the x-axis, outward flow is observed. In Figure 7, it can be observed that the magnitude of radial velocity decreases as the flow moves towards the outlets.

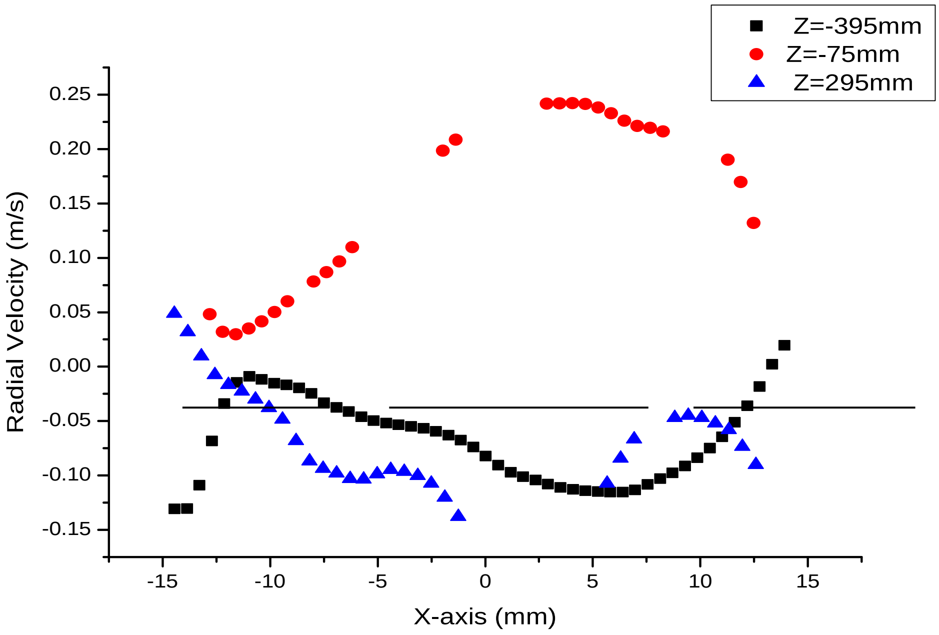

Figure 7: Comparison between the Radial Velocity Profiles at Three Axial Positions in the Cyclone

Conclusions

The stereoscopic PIV measurements were taken to investigate the single phase, water flow fields at three different axial positions within the pipe separator. Tangential velocity measurements showed that a forced vortex occurs at the center of the tube, with a free vortex near the wall region. The location of zero tangential velocity was observed to be off the axis of the pipe separator and the shape of the tangential velocity profile found to be independent of axial positions within the pipe separator. The tangential velocity profiles indicate that the magnitude of the mean tangential velocity decreases moving away from the inlet section to the outlets. The axial velocity measurements had shown the presence of fluid dynamic instabilities such as vortex breakdown and precessing vortex core caused by the high swirling motion inside the pipe separator. There is no general pattern for the radial velocity within the pipe separator. At the inlet section, the radial velocity was found to be directed outward. However, away from the inlet region, a pattern of both outwards and inwards flows was observed.

Acknowledgment

This research has been supported by the Petroleum Technology Development Fund (PTDF), Nigeria and Engineering and Physical Sciences Research Council (EPSRC) engineering instruments pool (TSI Inc.).

References

Afolabi, E. A. (2012). *Experimental investigation and CFD simulation of multiphase flow in a three phase pipe separator.* Unpublished Ph.D Thesis, Newcastle University, Newcastle, UK.

Erdal, F. M. (2001). *Local measurements and computational fluid dynamic simulations in a gas-liquid cylindrical cyclone separator.* Unpublished Ph.D. dissertation, The University of Tulsa.

Kelsall, D. F. (1952). A study of the motion of solid particles in a hydraulic cyclone. *Trans. Inst.Chem. Eng,* 30, 87- 108.

Leeuwner, M. J. & Eksteen, J. J. (2008). Computational fluid dynamic modelling of two phase flow in a hydrocyclone. *Journal of The South African Institute of Mining and Metallurgy,* 108 (4), 231-236.

Liu, Z., Jiao, J., Zheng, Y., Zhang, Q. & Jia, L. (2006). Investigation of turbulence characteristics in a gas cyclone by stereoscopic PIV. *AIChE Journal,* 52, (12), 4150 - 4160.

Melling, A. (1997). Tracer particles and seeding for particle image velocimetry. *Measurement Science and Technology,* 8, (12), 1406 - 1416.

Monredon, T. C., Hsieh, K. T. & Rajamani, R. K. (1992). Fluid flow model of the hydrocyclone: An investigation of device dimensions. *International Journal of Mineral Processing,* 35, (1-2), 65 - 83.

Peng, W., Hoffmann, A. C., Boot, P. J. A. J., Udding, A., Dries, H. W. A., Ekker, A. & Kater, J. (2002). Flow pattern in reverse-flow centrifugal separators. *Powder Technology,* 127, (3), 212 - 222.

Peng, W., Hoffmann, A. C., Dries, H., Regelink, M. & Foo, K. K. (2007). Reverse-flow centrifugal separators in parallel: Performance and flow pattern. *AIChE Journal,* 53, (3), 589 - 597.

Prasad, A. K. (2000). Stereoscopic particle image velocimetry. *Experiments in Fluids*, 29, 103 -116.

Prasad, A. K. & Jensen, K. (1995). Scheimpflug stereocamera for Particle Image Velocimetry in liquid flows. *Applied Optics,* 34 (30), 7092 - 7099.

Slack, M. D. & Wraith, A. E. (1997). Modelling the velocity distribution in a hydrocyclone. *4th International Colloquium on Process Simulation, 11–13 June, Espoo Finland,* 65–83.

Vazquez, C. O. (2001). *Multiphase flow separation in liquid-liquid cylindrical cyclone and gas-liquid - liquid cylindrical cyclone compact separators thesis.* The University of Tulsa.

Yazdabadi, P. A., Griffiths, A. J. & Syred, N. (1994). Characterization of the PVC phenomena in the exhaust of a cyclone dust separator. *Experiments in Fluids,* 17(1-2), 84 – 95.